DAA/LANGLEY

The College of William and Mary

Williamsburg, Virginia 23185

Semi-Annual Progress Report: December 15, 1984 - June 15, 1985

NASA Grant Number: NCC1-75

Title: Study of Static and Dynamic Stress Effects in Nonlinear Solids

Principal Investigator: Min Namkung

(NASA-CR-176236) STUDY OF STATIS AND DYNAMIC STRESS EFFECTS IN NONLINEAR SOLIDS Semiannual Progress Report, 15 Dec. 1984 - 15 Jun. 1985 (College of William and Mary) 19 p HC A02/MF A01 CSCL 20K G3/39

N86-10578

Unclas 15717

ABSTRACT

As the basic physical principles behind the low-field magnetoacoustic interactions have been unfolded, a new step in the present research had to be taken. For this, first, the stress measurements began in samples obtained from real railroad wheel and rail materials. Second, the effect of texture, which is the prime obstacle of conventional NDE techniques, has been investigated.

The first stage experimental results on these subjects again confirmed that the present technique is most suited for nondestructive stress characterization in steel components. The stress effects on the magnetoacoustic interaction obtained in a sample made from railroad rail were very similar to those obtained previously in 1045 steel. These results being somewhat different from the results with low (1020) and high (1095) carbon steels, there seemed to be certain range of medium carbon steels having the same characteristics. Also, as expected from the model, the stress information obtained by this technique has been confirmed to be least affected by the presence of texture.

I. INTRODUCTION

The magnetoacoustic technique has been shown to be able to differentiate the effects of uniaxial compression from those of others. This is because the initial slope of acoustic natural velocity with respect to net induced magnetization is negative only under compression when a steel sample is magnetized in the stress axis (1),(2). This phenomena is now very well understood in terms of basic physical mechanisms and a model description has been established (1). The importance of such a fact is that it is very feasible to apply this technique to determine the sign of bulk residual stress in ferrous alloy steels without having any calibration standard.

Previously, many different types of steel have been examined and the typical effects of compression has been found without any exception. There do exist, however, some variations in overall behavior of stress dependence of magnetoacoustic interactions according to the metallurgical properties of different types of steel. It was found that in 1020 and 1095 steel the stress effects were obtained exactly as were expected from the model, while 1045 steel showed some differences (1). Since railroad steel has carbon concentration of about .68 % which is close to that of 1045 steel, a similar stress effects were expected.

The presence of texture, commonly produced during the fabrication process, is known to impose the most difficult problem in nondestructive stress characterization. This is because the anisotropy of acoustic wave velocity due to texture is comparable to, or sometimes far greater than, that induced by uniaxial stress of reasonable magnitude. This is why even the determination of the sign of bulk residual stress has been possible only under very specific conditions when

conventional ultrasonic nondestructive techniuqe is used.

The low-field magnetoacoustic interaction is caused by the ferromagnetic domain structure change due to domain wall motion. The initial domain structure depends on many material factors. Among them is the structural property and is expected to affect the stress dependence of field induced accoustic natural velocity change in some way. The model, however, explicitly indicates that the structural property sholud not affect the general stress effect drastically but this fact is subjected to an experimental verification.

II. EXPERIMENTS AND RESULTS

The following experimental results were already presented in the meeting titled "Review of Progress in Quantitave NDE" at Williamsburg, Virginia in June, 1985 and will be published soon. Since the experimental procedures were identical to those reported so many times before, only the new results will be briefly outlined here.

A. Results with Railroad Rail Steel Sample

Figure-1 shows the stress dependence of $\Delta F(B)/F$ obtained by propagating 10 MHz compressional wave perpendicular to the stress axis which also was the magnetization axis. This type of steel is known to contain about .68 wt. % of carbon concentration. Figure-2 shows the results obtained previously with a 1045 steel rod under the same experimental arrangement. The common feature in these two figures is that the unstressed curves stay between tension and compression curves

which has not been found in 1020 and 1095 steels (1). In the previous report, such a peculiar stress effect was explained by assuming relatively high degree of microscopic local strains in this type of steel. More datiled experimental and theoretical study is planned to understand the stress effects in medium range carbon steels.

B. Results with a Severely Cold Rolled A-36 Steel Plate

Figure-3 shows the way the samples were cut, i.e. 0, 90 and 40-degrees with respect to the rolling direction. Lengthwise residual tension and compression were created by permanent bending with the final raidus of curvature of 25 cm. The experimental arrangements are shown in Figure-4. Next three figures show the $\Delta F(B)/F$ curves in these samples before and after permanent bending.

The shape of $\Delta F(B)/F$ curves obtained by Rayleigh surface waves depends on the ratio between the acoustic path lengths of material and delay line. As is shown in Appendix-1, the acoustic response on induced magnetization enhances as this ratio increases. The next three figures show the results obtained on sample surfaces under residual compression for various inter-transducer distances. The important point is the magnitude of $\Delta F(B)/F$ at its negative minimum under compression. This is almost the same in the 90 and 40-degree samples and is about half in the 0-degree sample. Hence, we conclude that the determination of the sign of residual stress is not affected by the presence of rolling texture.

III. CONCLUSION AND FUTURE PLAN

The experimental results confirmed that railroad steel is not an exception as far as differentiation of effects of uniaxial compression from those of tension by using the magnetoacoustic technique. As was expected, the behavior of $\Delta F(B)/F$ in this material was very similar to that obtained in 1045 steel. Another confirmation was made that the presence of severe cold rolling texture would not affect the unique capability of this technique, i.e. determination of the sign of residual stress without requiring a calibration standard.

The research work for the rest of the period will concentrate to construct a prototype measurement setup for the railroad industry. This effort will also be accompanied by a very detailed study on the effects of metallurgical properties on the magnetoacoustic interactions in steel. For this, a metallurgist from the Association of American Rails (AAR) has already joined this research program.

REFERENCES

1. M. Namkung, *Semiannual Progress Report*, Submitted to NASA LRC under the grant number NCCI-75, June, 1984.

2. M. Namkung and J. S. Heyman, *Proceedings of IEEE Sonic and Ultrasonics*, Vol. 2, 950, 1984.

List of Figures

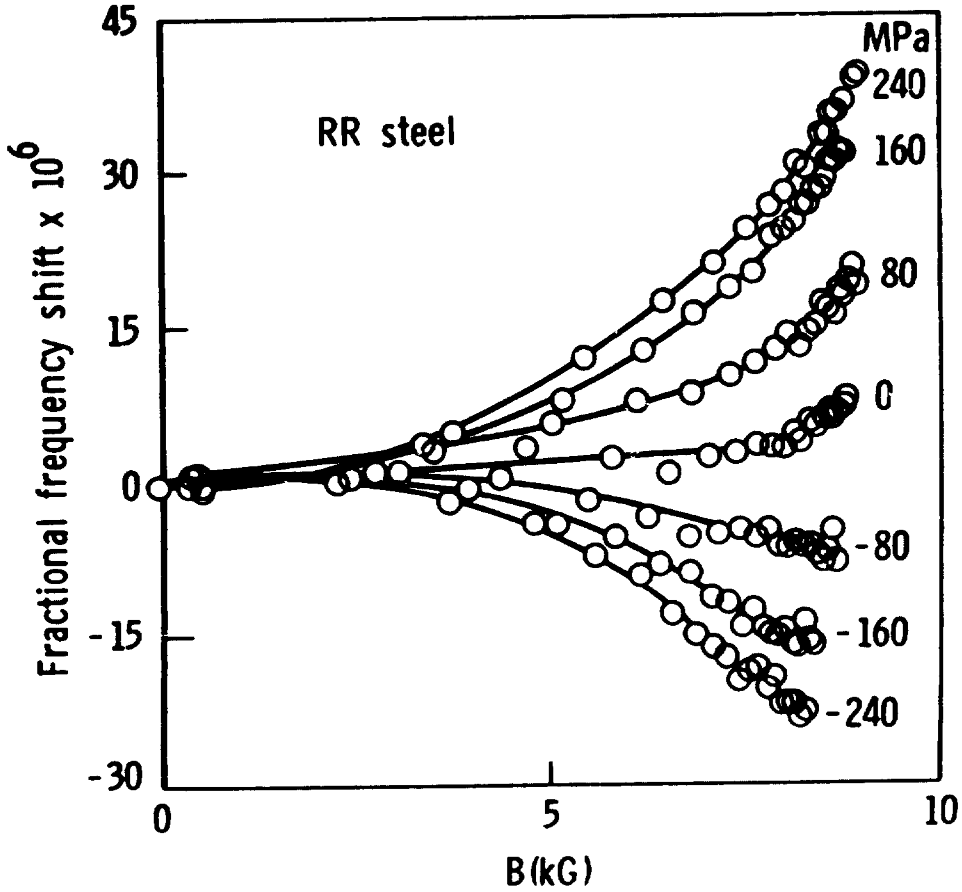
RR steel
MPa
240
160
80
0
-80
-160
-240
Fractional frequency shift x 10^6
45
30
15
0
-15
-30
0
5
10
B(kG)

Fig. 1

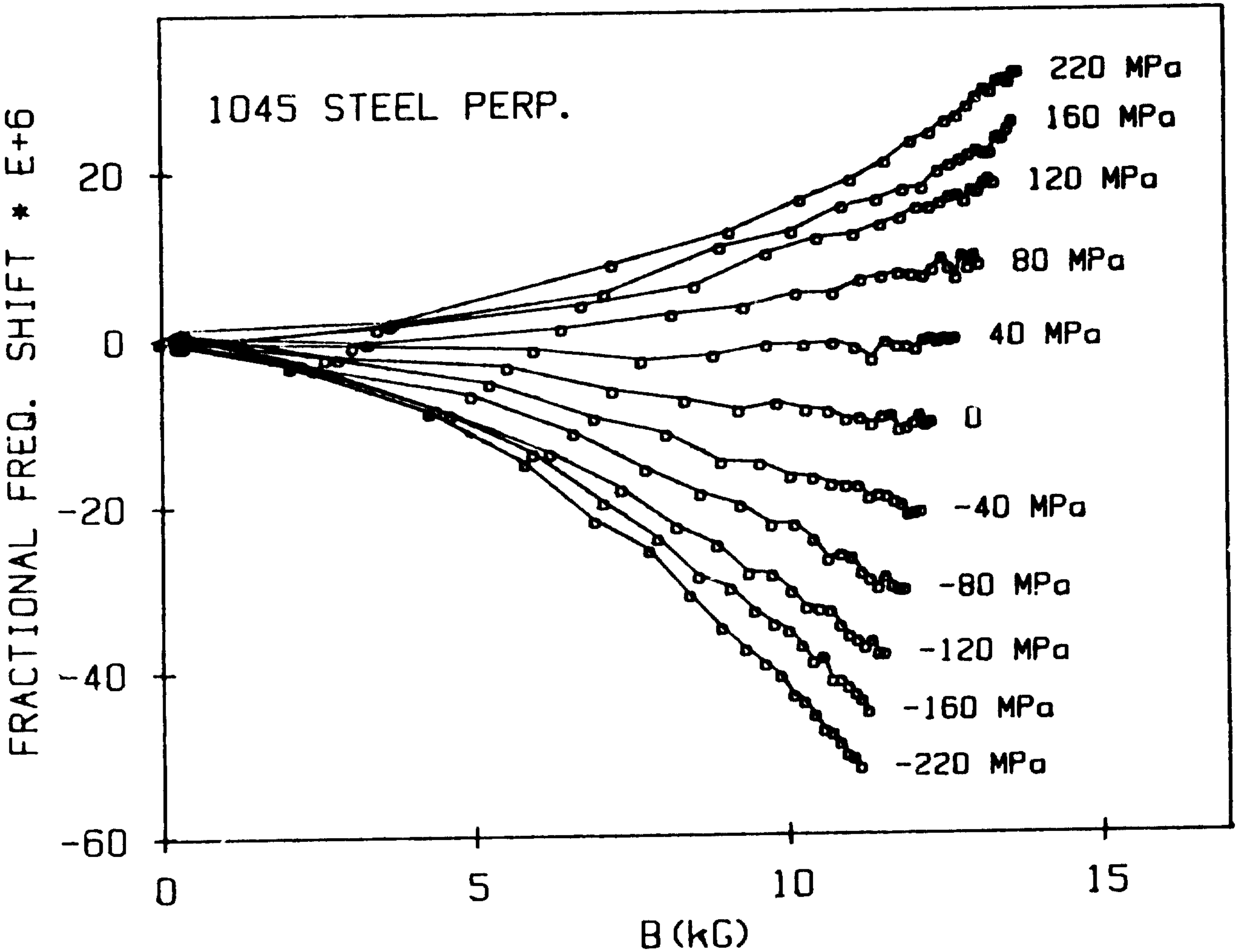
1045 STEEL PERP.
220 MPa
160 MPa
120 MPa
80 MPa
40 MPa
0
-40 MPa
-80 MPa
-120 MPa
-160 MPa
-220 MPa
FRACTIONAL FREQ. SHIFT * E+6
20
0
-20
-40
-60
0
5
10
15
B (kG)

Fig. 2

SAMPLE: HEAVILY COLD ROLLED A-36 STEEL PLATE

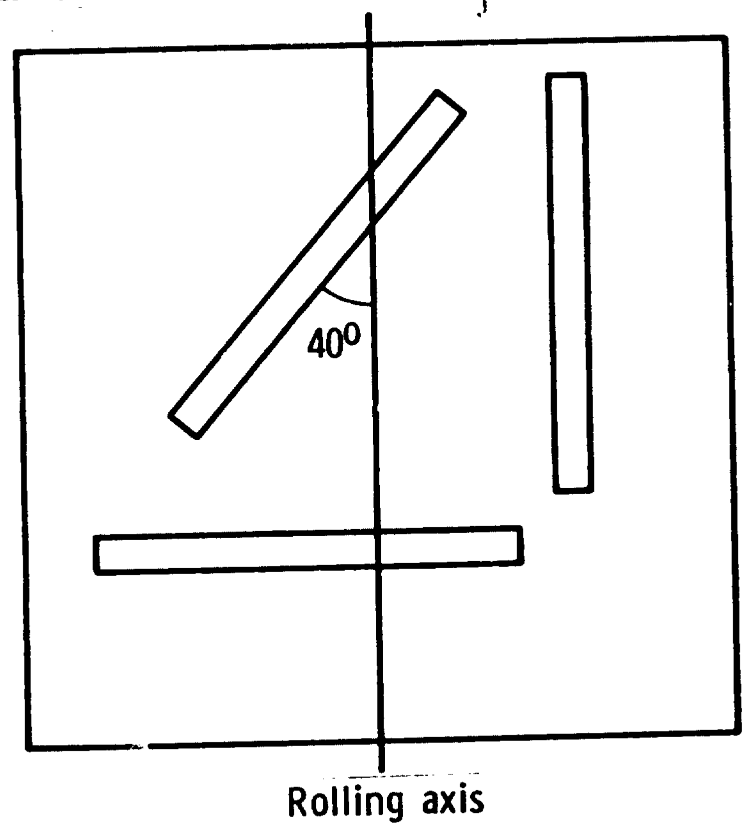

Fig. 3

EXPERIMENTAL ARRANGEMENTS

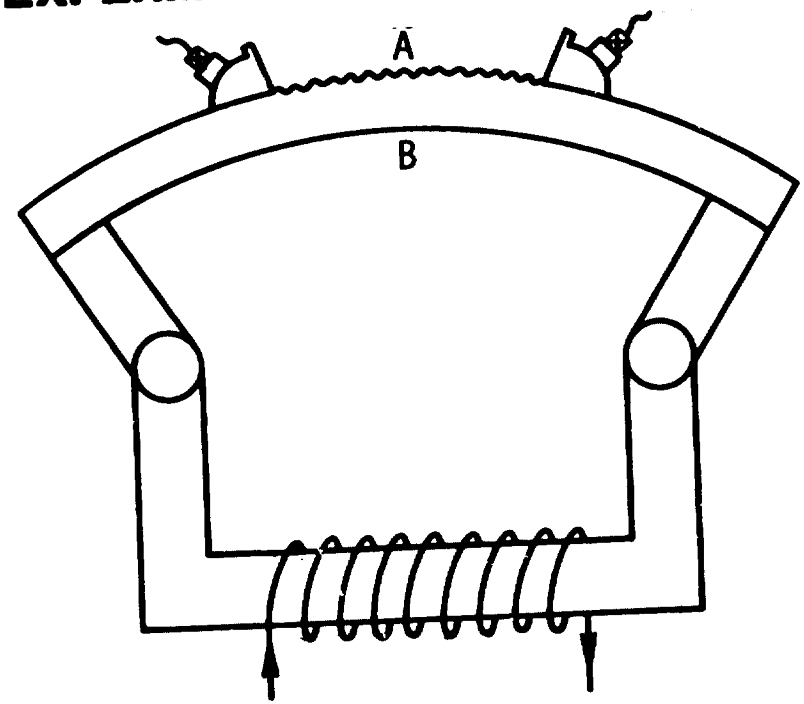

A: residual compression

B: residual tension

Fig. 4

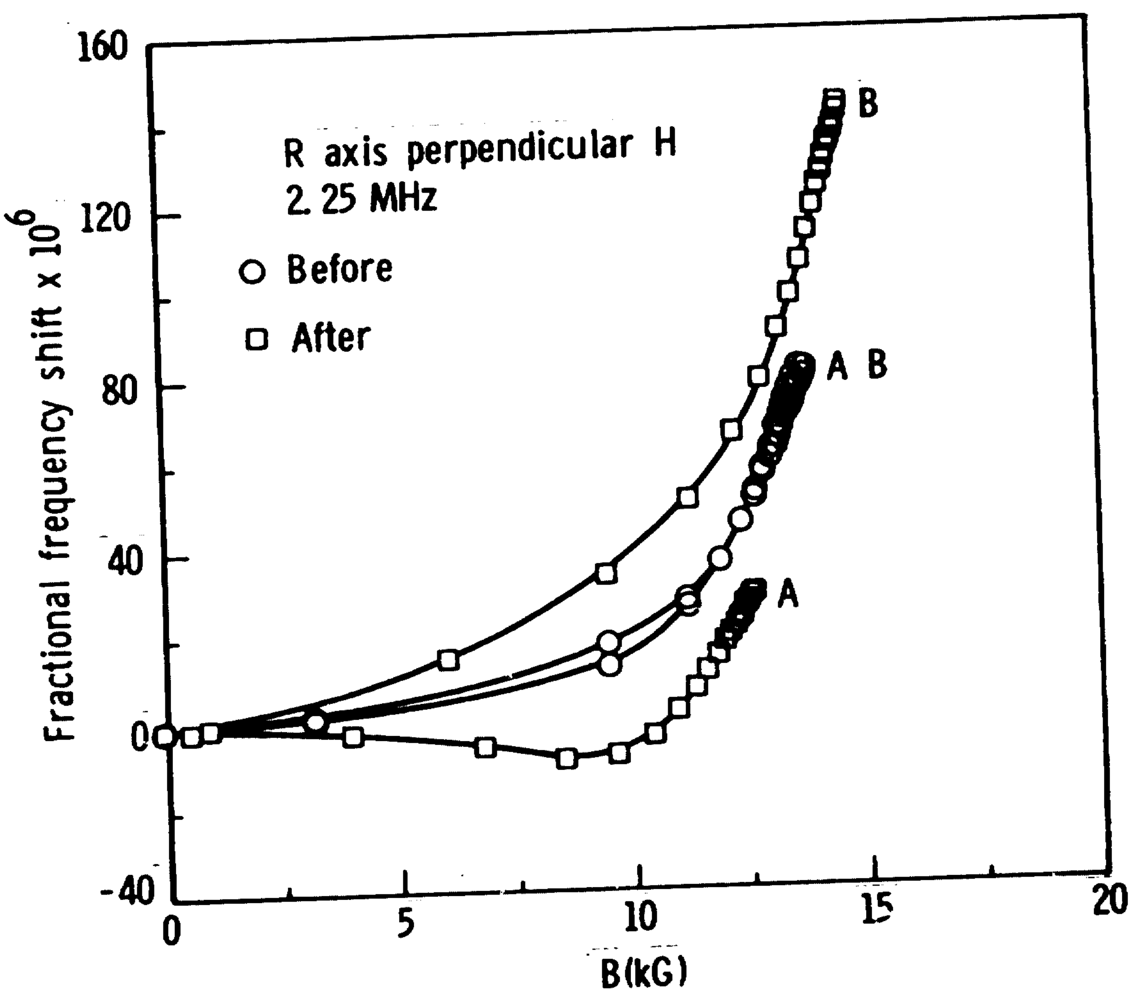
R axis perpendicular H
2.25 MHz
Before
After
A
B
A B
Fractional frequency shift x 10^6
160
120
80
40
0
-40
0
5
10
15
20
B(kG)

Fig. 5

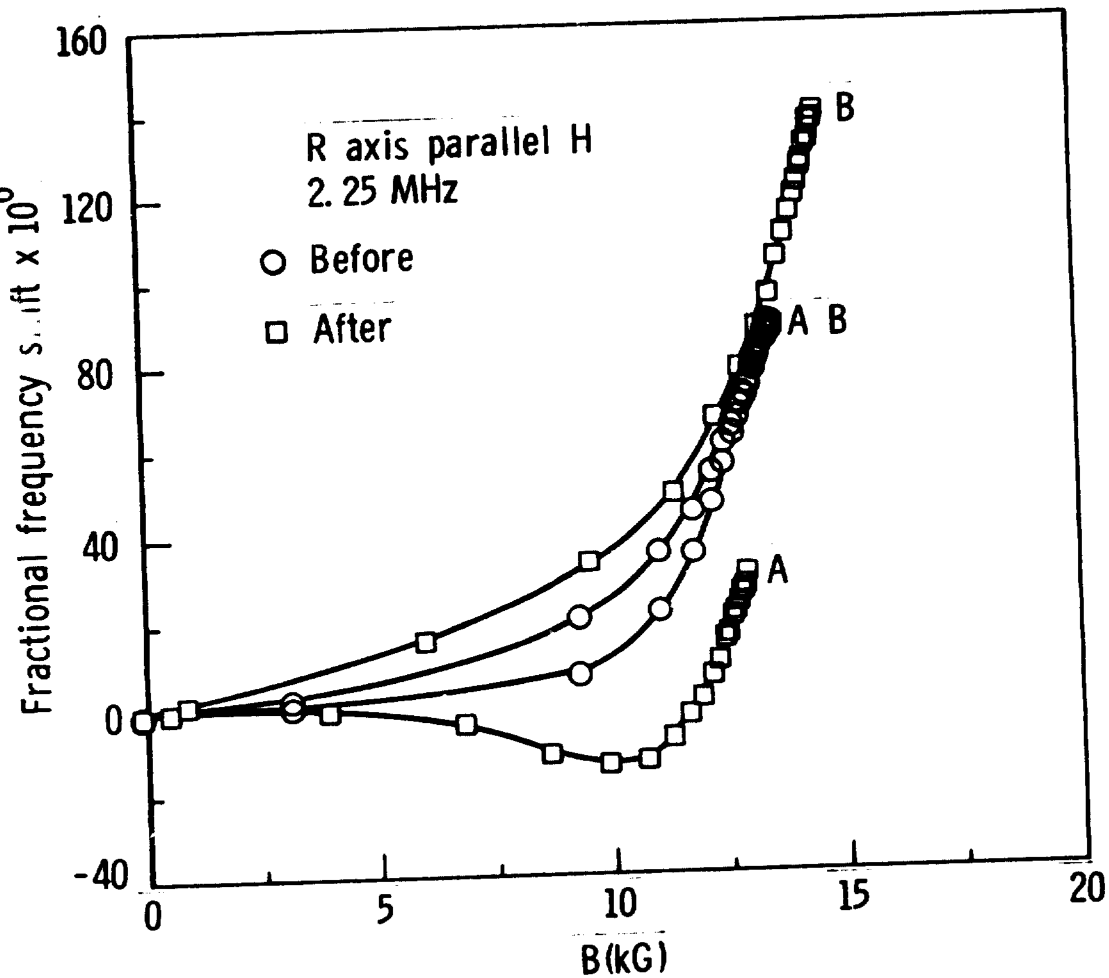
R axis parallel H
2.25 MHz
Before
After
A
B
A B
Fractional frequency s..ift x 10^6
160
120
80
40
0
-40
0
5
10
15
20
B(kG)

Fig. 6

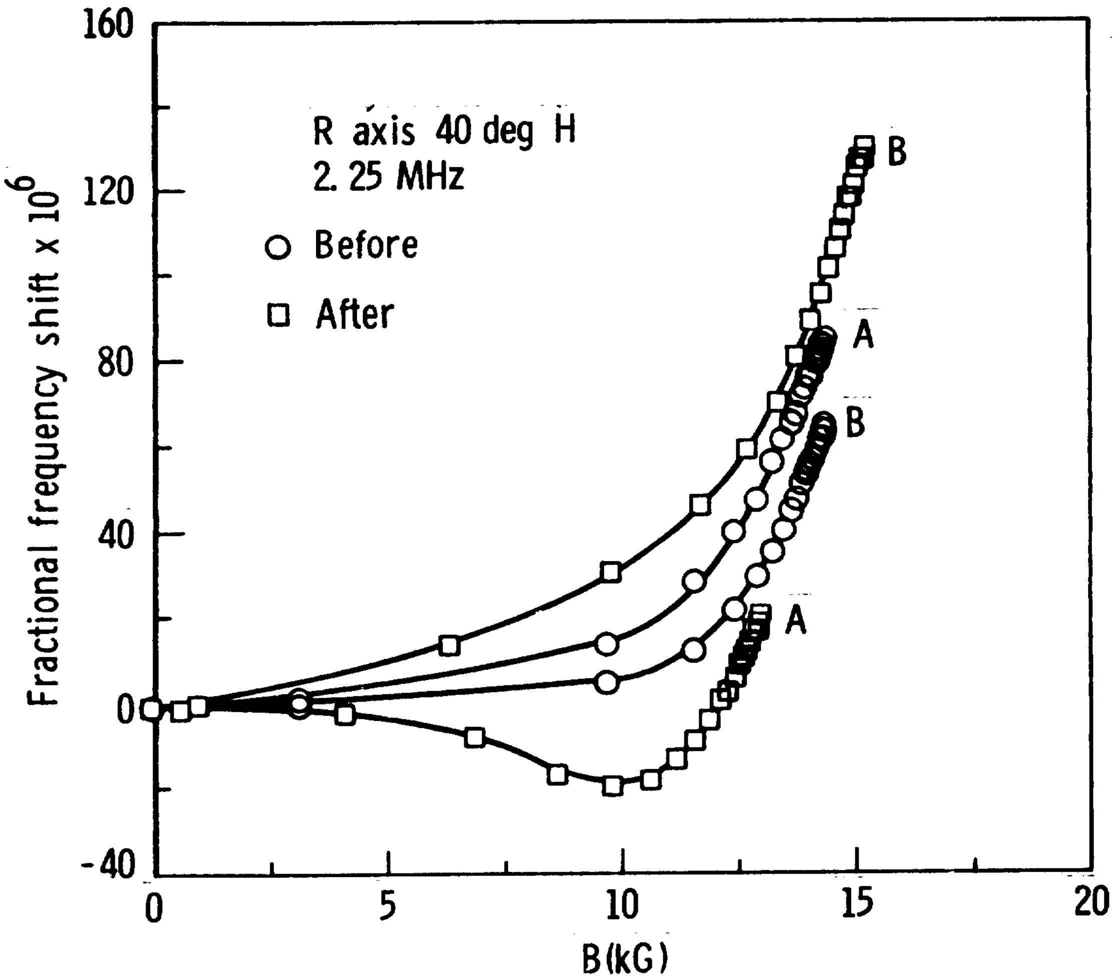
R axis 40 deg H
2.25 MHz
Before
After
A
B
A
B
160
120
80
40
0
-40
0
5
10
15
20
Fractional frequency shift x 10^6
B(kG)

Fig. 7

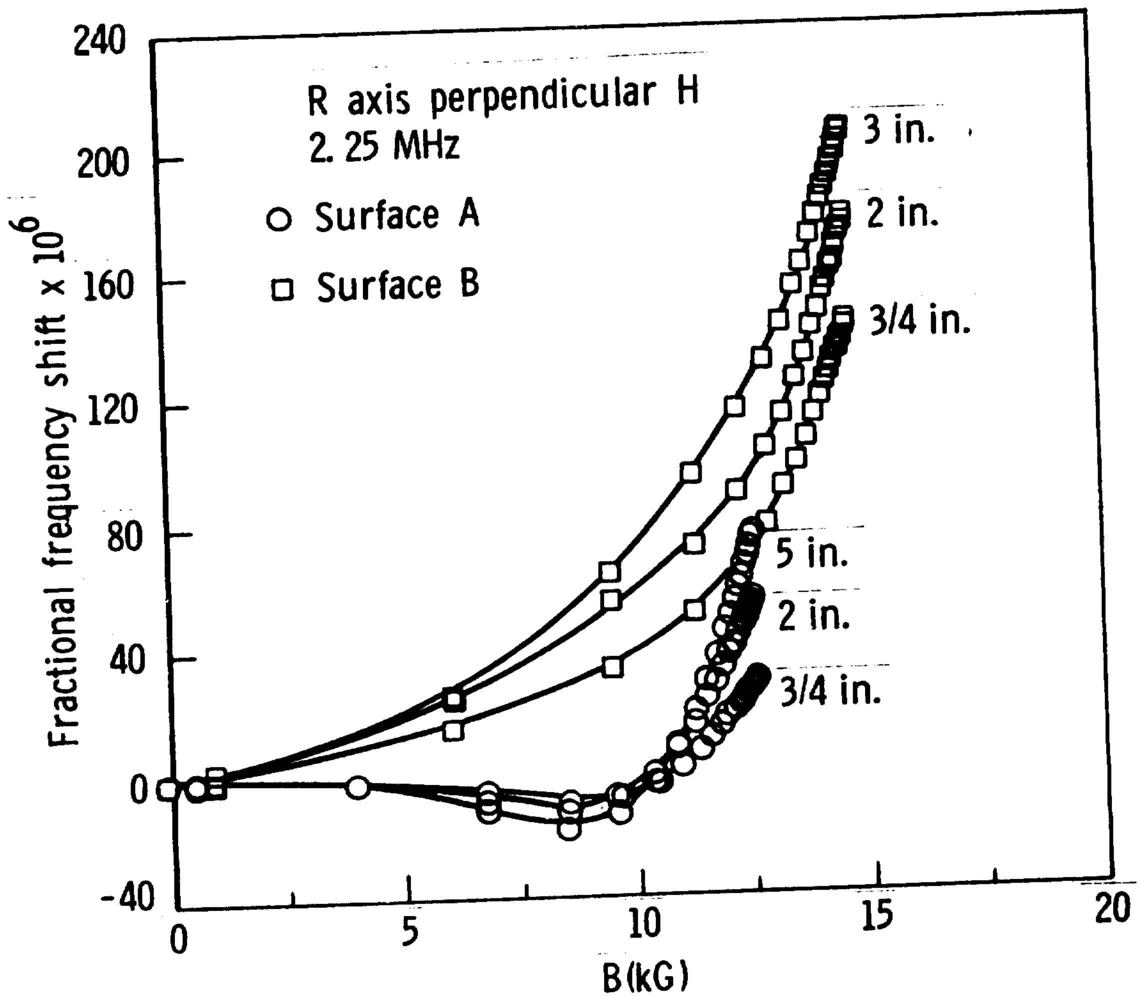
R axis perpendicular H
2.25 MHz
○ Surface A
□ Surface B
3 in.
2 in.
3/4 in.
5 in.
2 in.
3/4 in.
Fractional frequency shift x 10^6
240
200
160
120
80
40
0
-40
0
5
10
15
20
B(kG)

Fig. 8

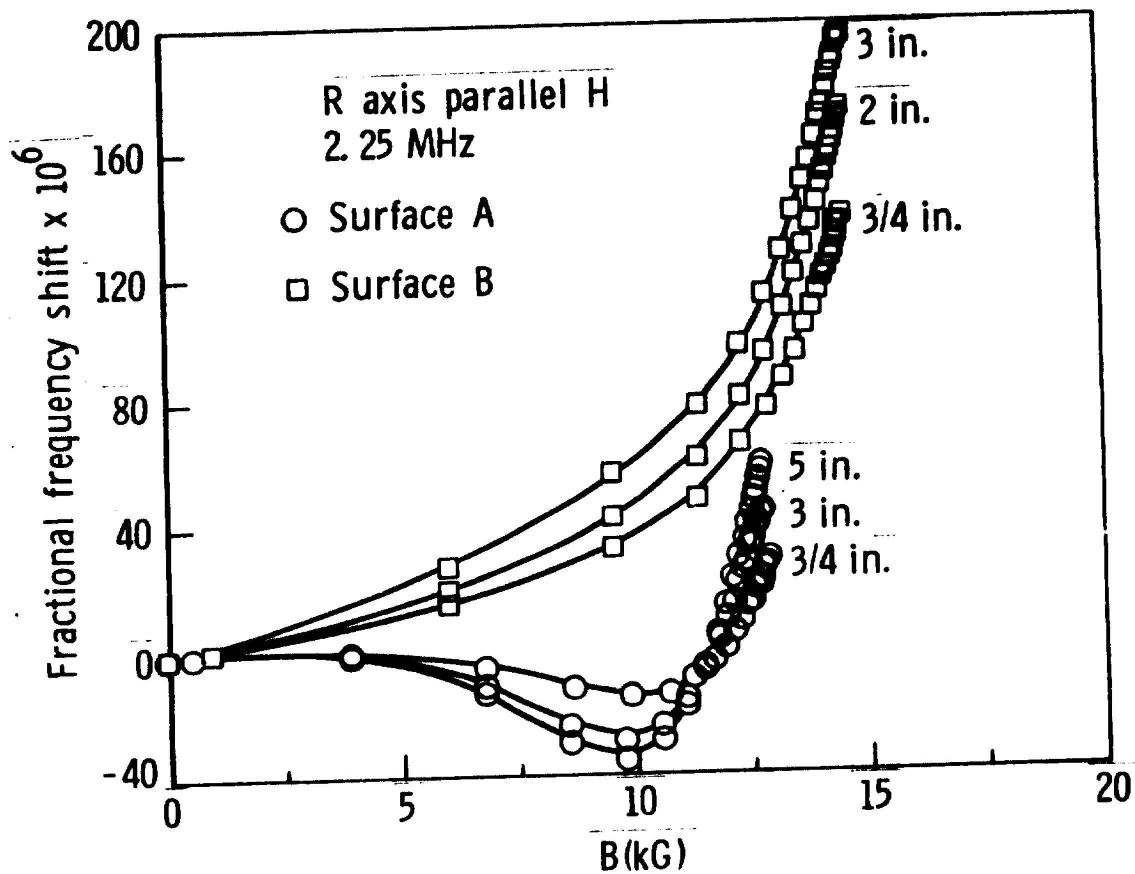
R axis parallel H
2.25 MHz
Surface A
Surface B
3 in.
2 in.
3/4 in.
5 in.
3 in.
3/4 in.
200
160
120
80
40
0
-40
Fractional frequency shift x 10^6
0
5
10
15
20
B(kG)

Fig. 9

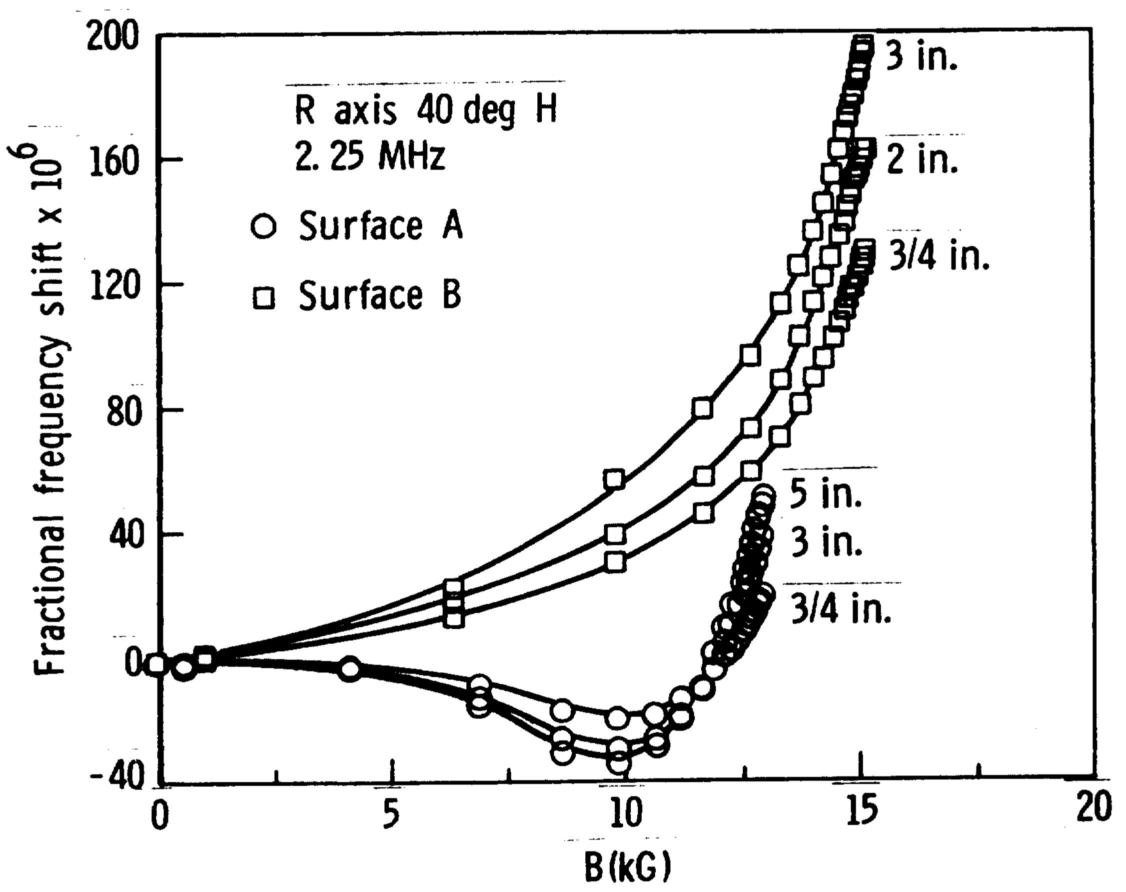
R axis 40 deg H
2.25 MHz
Surface A
Surface B
3 in.
2 in.
3/4 in.
5 in.
3 in.
3/4 in.
200
160
120
80
40
0
-40
Fractional frequency shift x 10^6
0
5
10
15
20
B(kG)

Fig. 10

EFFECT OF DELAY LINE LENGTH

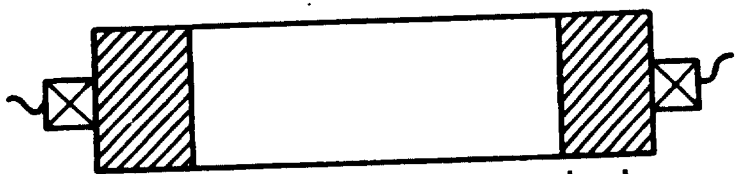

$$\frac{\Delta f}{f_o} = -\frac{\Delta t}{t_o} \text{ when phase-locked}$$

$$t_o = t_{mo} + 2t_d, \quad \Delta t = \Delta t_m$$

$$-\Delta t_m(B) = \alpha'(B) L_{mo} = \alpha(B) t_{mo}$$

$$\frac{\Delta f(B)}{f_o} = \frac{\Delta t_m(B)}{t_{mo} + 2t_d}$$

$$= \frac{\alpha(B) t_{mo}}{t_{mo} + 2t_d}$$

$$= \frac{\alpha(B)}{1 + 2t_d/t_{mo}}$$

$$= \frac{\alpha(B)}{1 + 2\frac{L_d}{L_{mo}}\frac{V_{mo}}{V_d}}$$

$$\sim \frac{\alpha(B)}{1 + 2L_d/L_{mo}} = \begin{cases} \alpha(B)/3 & \text{for } L_d/L_{mo} = 1 \\ \alpha(B)/1.4 & \text{for } L_d/L_{mo} = 1/5 \end{cases}$$

$V_d \sim 2700$ m/sec : lucite

$V_m \sim 3200$ m/sec : steel